Topics in Catalysis (2022) 65:1675–1685
https://doi.org/10.1007/s11244-022-01640-3

ORIGINAL PAPER

Spirulina Based Iron Oxide Nanoparticles for Adsorptive Removal of Crystal Violet Dye

Santosh Bhukal[1] · Anuj Sharma[1] · Rishi[1] · Divya[1] · Sumit Kumar[1] · Bansal Deepak[1,2] · Kaushik Pal[3] · Sharma Mona[1,4]

Accepted: 24 May 2022 / Published online: 28 June 2022

Abstract

In comparison to algal biomass, algae-based nanoparticle (green synthesis) not only aids in the removal of toxins from wastewater, but it is also an ecologically benign strategy with enhanced efficacy. In the present study, *Spirulina* is being utilised to make green iron oxide nanoparticles (S-IONPs), which further used to make an effective adsorbent for the removal of cationic crystal violet (CV) dye using ultra-sonic waves. The created nano-adsorbent was thoroughly investigated using a variety of characterisation techniques, including FT-IR, XRD, FE-SEM, and UV–VIS spectroscopy. Moreover, the S-IONPs adsorbent performed remarkably well in removing key chemicals from synthetic solutions, such as dyes. The pseudo-second order model was used to describe the kinetic profile, while the linearized Langmuir theory with r^2 of 0.96413 and q_{max} of 55.62 mg/g was used to show the adsorption isotherm. Sequestration of the CV dye from aqueous solution using S-IONPs was carried out efficiently. The potential of S-IONPs for decolorization of crystal violet dye solution was also confirmed through various analytical techniques.

Graphical Abstract

Preparation of *Spirulina* based iron oxide nanoparticles for sequestration of Crystal Violet dye from aqueous solution

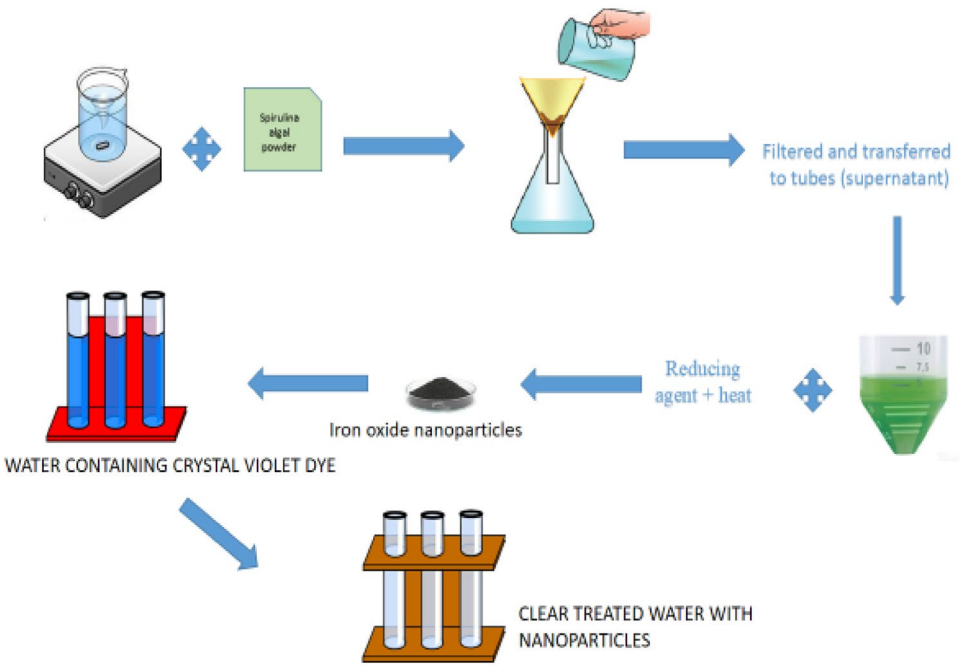

Keywords CV dye · Nano-adsorbent · Removal efficiency · Algal iron oxide NPs

Extended author information available on the last page of the article

1 Introduction

Environmental contamination is currently a topic of significant attention and concern around the world owing to the harmful consequences it has on living creatures and ecological units [1]. These issues are getting worsen because of the fast growth of industrialisation across the world [2, 3]. Pollution causes several problems, including respiratory issues, cardiovascular illness, intestinal damage, the decreased standard of life, climate change and the disappearance of many plant and animal species [4]. Water is regarded as one of the most fundamental, crucial, and irreplaceable aspects in the survival of human beings and ensuring the long-term growth of human civilisation on our planet. Water contamination associated with explosive industrialisation has become the most problematic issue in environmental concern in recent decades, arousing significant global concern due to their severe effects on a variety of living beings [5]. Scarcity of water is affecting an estimated 2 billion people, and around 800 million people are not having access to potable water, resulting in major health consequences [6, 7]. Among the many manufacturing units that contaminate water, the clothing industry is the major one that dumps the most refuse into it; this industry utilises over ten thousand dyes and pigments in its shading operations, mostly non-biodegradable in nature [8]. The exact number of dyes and their amount expelled by the clothing industry into oceanic effluents are unclear, but this pollution is a major ecological concern [9]. The most often used dyes in the textile sector are Rhodamine b, Methyl orange, and Methylene blue and Tri-phenylmethane dye, Crystal Violet [10, 11].

Crystal Violet (CV) is a tri-phenylmethane dye that is widely utilized as a staining agent in biological activities, a dermatological agent, and in a variety of viable textile applications [12]. Hexamethyl pararosaniline chloride is also one of its names and it is an elementary dye with the molecular formula $C_{25}H_{30}N_3Cl$. The dye was discovered to be poisoning at the mitotic stage that is recalcitrant and cancer causing, and it is thus classified as a risk to human health [13]. Its removal from wastewater before disposal is thus critical for environmental safety.

The retention of dyes and/or their degradation products in aquatic bodies harm the health conditions of many living organisms. These deteriorate the quality of water (specification) by altering the concentration of parameters like BOD, COD, TSS, and TDS resulting in a net loss of photosynthetic activity by increasing turbidity combined with inadequate light penetration [14]. Several governments have imposed environmental limits on the quality of coloured wastewater, requiring enterprises to remove dyes from their effluents before dumping [15]. However, traditional wastewater treatment facilities have proven to be very unsuccessful in removing commercial dyestuffs from wastewaters, particularly CV dye and they are directly or indirectly caused harm to nature. So there is a need for sustainable treatment technology that efficiently removes contaminants like dye from wastewater and is also eco-friendly in nature [16].

Some bio-sorbents, such as *Chlorella vulgaris* [17], *Ulothrix sp*. [18], *Ananas comosus* leaf powder [19], and *Scolymus hispanicus* [20], have been efficiently utilized in biomass form to eliminate dyes from wastewater, according to the literature. However, *Spirulina* biomass is often used to eradicate metals such as lead, cadmium, nickel and copper [21–23] while research on dye removal onto *Spirulina* are few. This research is oriented to finding biocompatible *Spirulina* assisted algal nanoparticles with tuneable features having improved efficiency. As in above mentioned literature, algal biomass is used as an adsorbent for wastewater removal but algal NPs have a high surface area in comparison to biomass. Nanoparticles have higher reactive sites for the formation of hydrogen bonds. Therefore, nano sized algal adsorbents catalysis the reaction by providing more surface area for adsorption, as illustrated in Fig. 1. Functionalization of the surface enhances the adsorption capacity of particles.

Spirulina is a filamentous cyanobacterium (blue-green alga) that is cultured and sold globally among a range of microalgae species. They may grow phototrophically, heterotrophically, or mixotrophically in a variety of environments including freshwater, seawater, and pond water under harsh living circumstances such as low light and the presence of organic materials and pollutants. Along with wastewater treatment biomass of *Spirulina* can also be used in the pharmaceutical industry, and biofuel production [24]. The use of algal biomass as a nanoparticle (NPs) to remove dyes is rarely studied. Synthesis of nanoparticles with the help of algae is an eco-friendly approach to wastewater treatment and it efficiently removes various pollutants like dye and heavy metals from wastewater. The potential of NPs of *Spirulina* biomass as bio-sorbents for CV dye removal was examined in this study.

Nanotechnology is a promising and rapidly expanding field of research that is bridging gaps in contemporary important technologies. Nanotechnology has advanced in the field of nano-science over the last two decades. NPs are small particles with diameters ranging from 0 to 100 nm [25]. The constructional distinctiveness of NPs, such as size, form, and lattice, has boosted their use in electrical devices, bio-engineering, pharmaceutical, and textile sectors, as well as biomarkers and biosensors [26–29]. Among the various physical and chemical methods (e.g., microemulsion, sol–gel method, electrochemical, and so on) used for the synthesising NPs, the less toxic synthesis of NPs in terms of eco-friendly synthesis using plant extracts (e.g.,

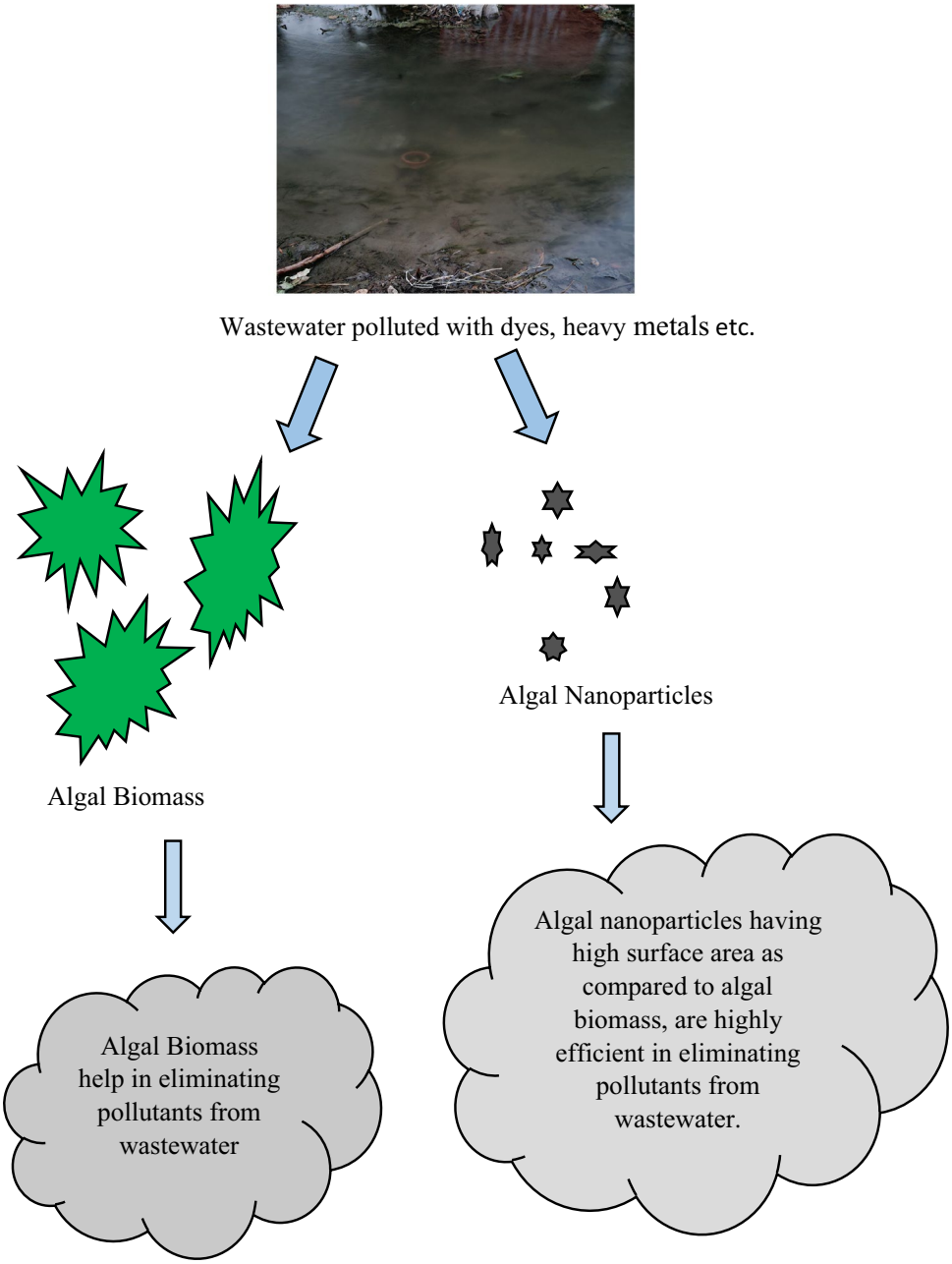

Fig. 1 Schematic illustration of the advantage of using algal nanoparticles over algal biomass in wastewater treatment

fruit and leaf) or biological organisms (fungi, bacteria, yeast, seaweed) is now evolving because of its cost-effectiveness, high production rate, and environment-friendly nature [30]. These materials contain a wide range of bioactive components (for example, carbohydrates, amino acids, proteins, vitamins, alkaloids, saponins, polyphenols, steroids, organic acids, flavonoids, terpenoids, and reducing sugars), which are used as capping, reducing, and stabilising agents during the process of NPs synthesis [31].

Most of the algal nanoparticles studies revolve around gold (37%) & silver (39%) and very few studies focused on other metallic and metal oxide nanoparticles [32]. Therefore, this study aims to get more out of the commercially available sustainable *Spirulina* algae powder by greenly synthesising iron oxide NPs and systematically testing its capacity to decolourise CV dye from wastewater. Also in this field, researchers need to explore the type of nanoparticles, their suitable size and their potential to act as a biosorbent at the nanoscale. The first section of this article concentrates on several structural characterization investigations (physical and chemical characteristics) of the as-formed S-IONPs, including X-ray diffraction (XRD), Fourier-transform infrared spectroscopy (FTIR), High Resolution Field Emission Scanning Electron Microscopy (FE-SEM) and UV–VIS

spectroscopy. In the Second section, the efficacy of S-IONPs was tested for the removal of CV dye and was examined under working parameters (i.e., sorbent concentration, pH of the solution, contact time, dye concentration, and temperature) in order to get a systematic knowledge of the interaction of dyes and nano-adsorbent, which is required for application on large-scale, including customization of as synthesised nano-adsorbents, the assortment of an appropriate adsorbent and defining of an optimal eluent.

2 Materials and Methods

2.1 Materials

In the present study, the chemicals used were of standard methodical mark and were used straight without any refining. Chemicals used were powdered form of microalgae, ferric chloride hexahydrate ($FeCl_3{\cdot}6H_2O$), methanol (CH_3OH) and ethanol (C_2H_5OH) and salt of CV dye. Different solutions were prepared using deionised water (DI). pH of all dye solutions were controlled by using diluted HCl and NaOH of 0.1 M.

2.2 Iron Oxide Nanoparticles (S-IONPs) Synthesis

2.2.1 *Spirulina* Micro-algal Supernatant Preparation

Microalgal Powder (MALGP) of *Spirulina* was firstly splashed with normal tap water and then rinsed with DI water to eliminate observed impure particles as per Fig. 2. The 12 g microalgal Powder of *Spirulina* was dissolved in 120 ml of DI water in a 500 ml round-bottomed flask by stirring continuously using a magnetic stirrer for 1 h. The homogenized solution is allowed to cool down naturally at 25 °C, the MAGLP was strained through a filter paper (whatman paper of diameter 125 mm) and the clear supernatant solution was transferred in polypropylene tubes and set aside for the synthesis of *Spirulina* iron oxide nanoparticles (S-IONPs).

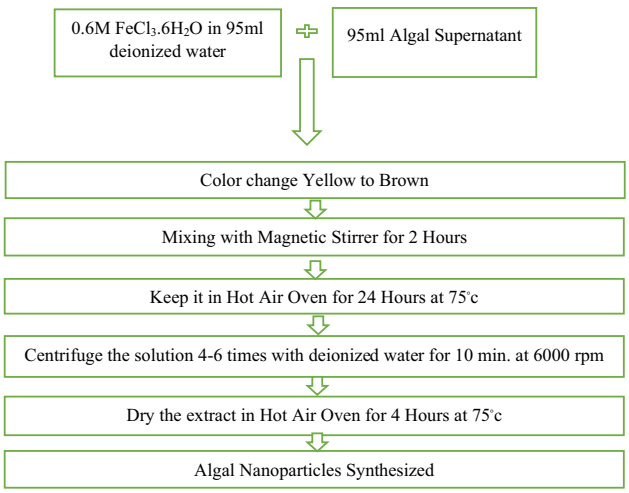

Fig. 2 Flow diagram showing the basic procedure for synthesis of S-IONPs

2.2.2 *Spirulina* Iron Oxide Nanoparticles (S-IONPs) Preparation

The best synthesis condition was continued by referring to the literature reported.

2.3 Preparation of Dye Solutions

Dye standard stock solution of 1000 ppm concentration was prepared for different sorption experiments. A suitable amount of CV dye salt is dissolved in a suitable amount of DI water to prepare the solution and left for stirring at approx. 100 rpm for 20 min to ensure dissolution. Further parameters were done with the stepwise dilution of stock solution.

2.4 Physical Characterisation of S-IONPs Sorbent

Fourier-transform infrared spectroscopy analysis of NPs inside the algal extract solution was utilised to determine the efficient groups of the active components. The FTIR spectrophotometer model used was Perkin Elmer spectrum, a standard optical system with KBr powder, 4000–500 cm^{-1} is the spectral range used for the collection of data, at the highest resolution of 0.5 cm^{-1}. Identification of the spectral absorption bands was made according to previously published information. XRD (Benchtop Miniflex- II, Rigaku, Japan) was performed to identify the structure of the S-IONPs ($\lambda = 1.54056$ A) between 10° and 90° (2θ) at 27 °C. FE-SEM was performed using model/maker-7610F Plus/JEOL. UV–Visible spectroscopy of S-IONPs was performed using a UV–VIS-NIR spectrophotometer (Varian cary-5000) in the range of 200–800 nm wavelength.

2.5 Sorption Assay Experiments

S-IONPS absorption performance towards CV dye is checked by batch equilibrium scheme. For the studies of sorption, out of all the operational parameters one parameter is kept varying comprehensively, while others kept running the same continuously.

To check the influence of initial solution pH (pH_i), 0.03 g of S-IONPs was mixed with a sequence of 20 ml of CV having different pH values vacillating from 2 to 14 maintained with the use of 0.1 M of diluted HCl and NaOH. The tested solutions were constantly stirred under sustained conditions for a

contact time of 100 min and a stirring speed of 200 rpm. After that sorbent was loaded with CV dye magnetically collected from the solution and the residual supernatant was estimated for the remaining dye concentration at 464 nm wavelength using the Shimadzu- UV-1280 Multipurpose UV–Visible Spectrophotometer. The impact of adsorbent concentration was investigated by altering the concentration S-IONPs from 10 to 110 mg with a 20 ml dye solution. It is further quantified using spectrophotometry. Kinetics investigation was led as an exercise of contact time by dissolving 0.75 g S-IONPs with 500 ml of dye solution for 120 min and stirred at 200 rpm. Samples were collected at stipulated time intervals and further processed. The isotherm studies were performed by dissolving 0.03 g of S-IONPs with 20 ml dye solution with varying dye concentrations ranging from 10–100 ppm. The temperature effect was noted by mixing 0.03 g of S-IONPs in 20 ml dye solution at different temperatures.

2.6 Kinetics Modelling Analysis

Sorption kinetics study is important to get a full understanding of sorption reaction, saturation time and all the steps which probably control the sorbate and sorbent interaction. This is important for the large scale implication of the sorption system. To understand the nearest fitted kinetics models, the resulted data was handled with two models: pseudo first-order rate equation (PFORE) [33], pseudo second order rate equation (PSFORE) [34]

2.7 Different Adsorption Isotherm Models

The adsorption data were examined additionally using well-known isotherm models such as Langmuir and Freundlich equilibrium isotherm models. The equilibrium concentration of dye is C_e (mg/L), the quantity of adsorbed dye is Q_e (mg/g), and the adsorption capacity and energy are q_{max} (mg/g) and b (L/mg), respectively. If the system follows the Langmuir model, the plot of C_e/Q_e vs. C_e will be linear. The empirical constants of (mg/g) and n are defined. Multiplayer adsorptive activity of dye over S-IONPs is facilitated by electrostatic attraction caused by the existence of functional groups on dye molecules and surface alter NPs. Using the q_{max} values derived from the Langmuir model, the highest adsorption potential was in comparison with the varied surface coverage of S-IONPs [35].

3 Result and Discussion

3.1 Characterization of *Spirulina* Mediated Iron Oxide Nano sorbent

3.1.1 Fourier Transform Infrared Spectroscopy (FT-IR)

In general, the FT-IR scale is used to distinguish the binding groups entangled in the adsorption. The spectrum of *Spirulina* mediated iron oxide nano-adsorbent is shown in Fig. 3. The wide attributed adsorption band at 3436.73 cm^{-1} represent O–H bonding for alcohol (–OH) or carboxyl group (–COOH). A small signal band observed at 2065.00 cm^{-1} represents the C≡C bonding. The sharp peak detected at 1636.87 cm^{-1} represents the aromatic stretching vibration of C=C bonding which is found in alkene groups. A weak signal peak observed at 1404.1 cm^{-1} show the C–H bonding with sp^3 hybridization. Another peak observed at 1384.90 cm^{-1} is related to symmetric nitro and stretching of the C–H bond of alkanes group with sp^3 hybridization. The vibration peak observes at 1045.2 cm^{-1} represents the C–N bonding and C–O bonding of alkoxy groups. The peak observed at 576.16 cm^{-1} confirms the synthesis of iron oxide nano-adsorbent made up with the help of *Spirulina* because the peak represents the widening of the metal–oxygen group. These peaks are almost identical to the previous study by various researchers [31, 36, 37].

The FT-IR spectrum of *Spirulina* mediated iron oxide nano-adsorbent with the loading of CV dye is shown in Fig. 4. The new peak that appeared at 2928.1 cm^{-1} represents the C–H bonding of alkane groups with sp^3 hybridization and stretching O–H bond of the carboxyl group, while another peak at 2853.6 cm^{-1} signifies the weak bond of C–H in aldehyde groups with sp^3 hybridization. The sharpest peak observed at

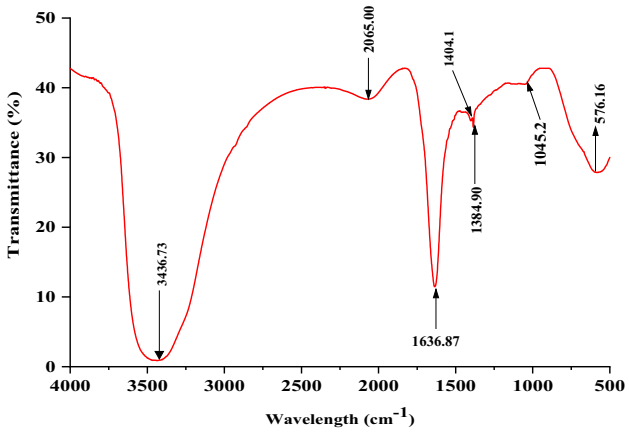

Fig. 3 FT-IR spectrum of iron oxide nano-adsorbent synthesised with *Spirulina*

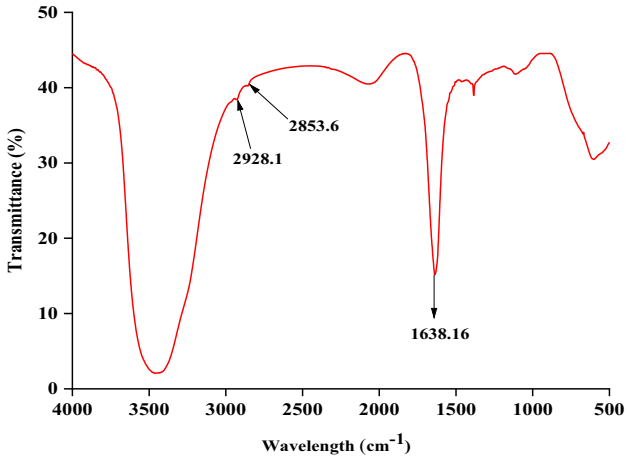

Fig. 4 FT-IR spectrum of *Spirulina* mediated iron oxide nano-adsorbent loaded with CV Dye

1638.16 cm^{-1} represents the saturated amide group with C≡O bonding. These peaks confirm the adsorption of CV dye on iron oxide nano-adsorbent made up with the help of *Spirulina* [31, 38].

3.1.2 X-ray Diffraction (XRD)

XRD was performed to investigate the crystalline nature and phase of synthesized nano-adsorbent. XRD of iron oxide nanoadsorbent synthesized using S*pirulina* is represented in Fig. 5. The characteristic peak of S-IONP is best observed at 26.63° on (2θ). The crystallite size of the nanoadsorbent is calculated using the Debye–Scherrer equation [39],

$$d = K\lambda/\beta \mathrm{Cos}\theta \quad (1)$$

where d denotes the crystalline size of nanoparticles, k is a constant dimensionless value which is known as the shape factor**,** λ is the wavelength of incident X-ray, Bragg's angle in radians is denoted by θ, and β refers to the full width at half maximum (FWHM) [40]. The average size of S-IONP calculated using the Debye–Scherrer equation is 28.497 nm. A similar kind of result was observed when iron oxide nano-adsorbent was synthesized using a composite of *Psidium guavaja-Moringa oleifera*, *Teucrium polium and Bauhinia tomentosa* [39–41].

3.1.3 Ultra-Violet/Visible Spectroscopy

For observing the optical properties of synthesized nano-adsorbents, they are characterized through UV–VIS spectroscopy. Figure 6 represents the absorption peak observed during UV–VIS spectroscopy of synthesized nano-adsorbents. The absorbance peak of iron oxide nanoparticles is between 280 and 400 nm [41], in our study a broad peak was found between 300 and 400 nm, thus signifying the synthesis of iron oxide nanoparticles. A similar kind of peak was observed in other studies when iron oxide nanoparticles were synthesized with the help of *Spirulina platensis* (absorbance peak at 405 nm), a composite of *Psidium guavaja-Moringa oleifera* (absorbance peak at 310 nm) and *Eichhornia crassipes* (absorbance peak at 379 nm) [31, 39, 40].

3.1.4 FE-SEM Analysis of S-IONPs

The FE-SEM images of S-IONPs with different magnifications of ×1000, ×10,000, ×15,000, and ×20,000 has been observed and shown in Fig. 7. This image shows nanoparticles are accumulated, have non-uniform (non-regular) structures and are almost distinctive. Nanoparticles are gathered together because of magnetic interaction (dipole–dipole)

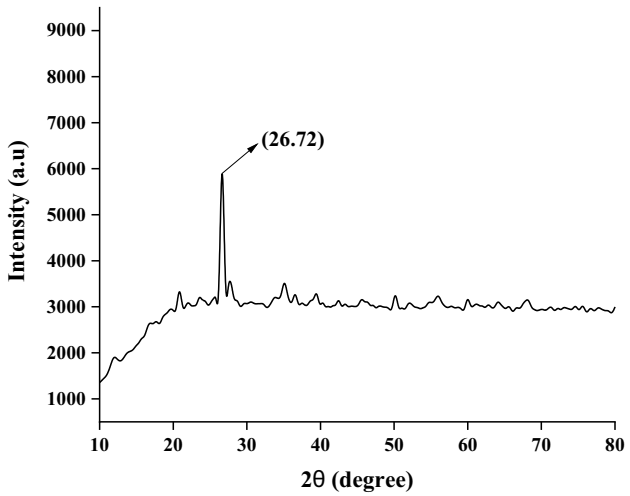

Fig. 5 XRD of iron oxide nano adsorbent synthesized using *Spirulina*

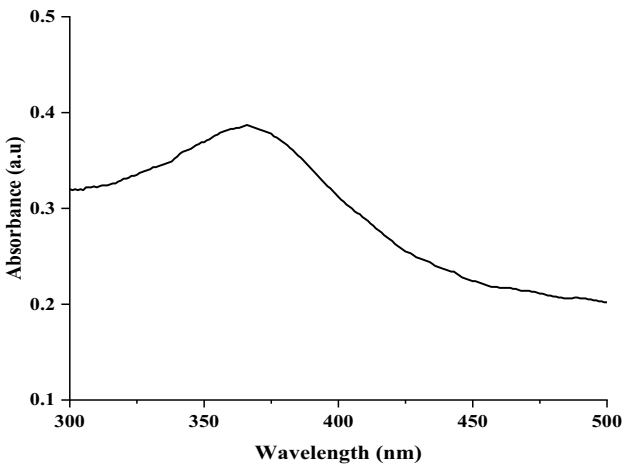

Fig. 6 UV–VIS Spectroscopy measurement of S-IONPs

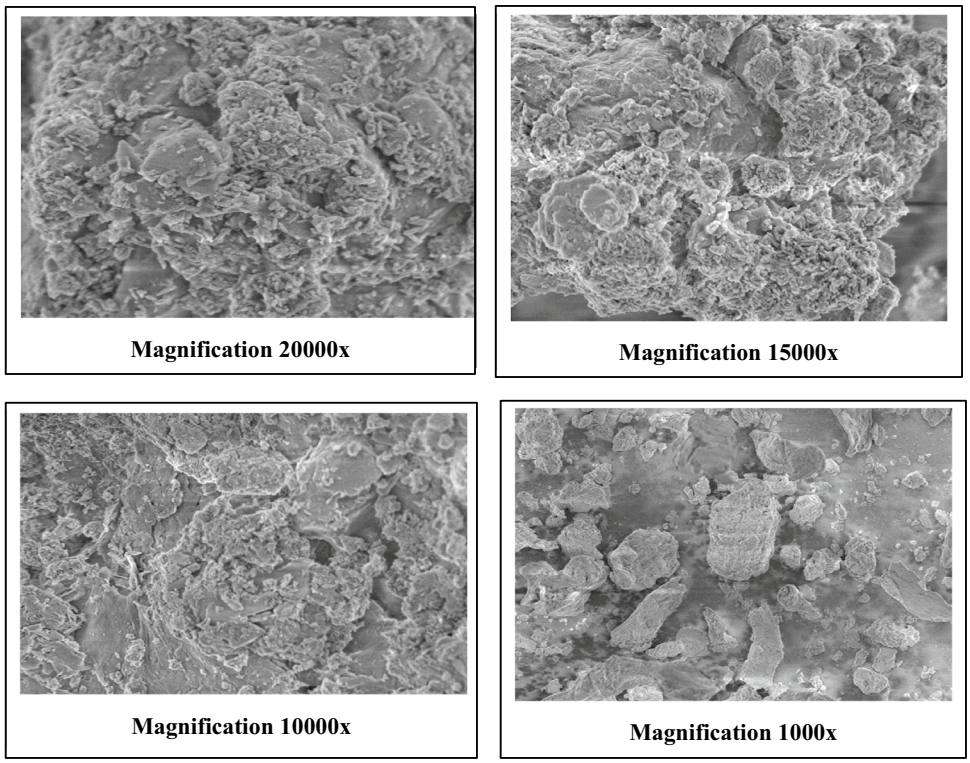

Fig. 7 FE-SEM analysis of *Spirulina* mediated iron oxide nanoparticles

between species of iron. Morphology and size of S-IONPs can be greatly influenced by the presence of various bioactive reducing agents like polyphenols in microalgal powder supernatant. Some clumped clusters are also shown in the figure because small bioactive compounds stick together to form these clusters [31, 39, 42–44]. EDX analysis of S-IONPs (Fig. 8) confirms the presence of Fe, O, Cl, and C. The weight % of elements is Fe (25.4%), O (43.2%), Cl (4.9%) and C (26.5%).

3.2 Impacts of Varying Operative Parameters

3.2.1 Impact of pH

pH is one of the significant parameters because it directly influences the sorption properties of nano-adsorbents [45]. The dye elimination efficiency of nano-adsorbents was found to be continuously increasing as pH increased from 2 to 12. At pH 2 the dye elimination efficiency of nano-adsorbents

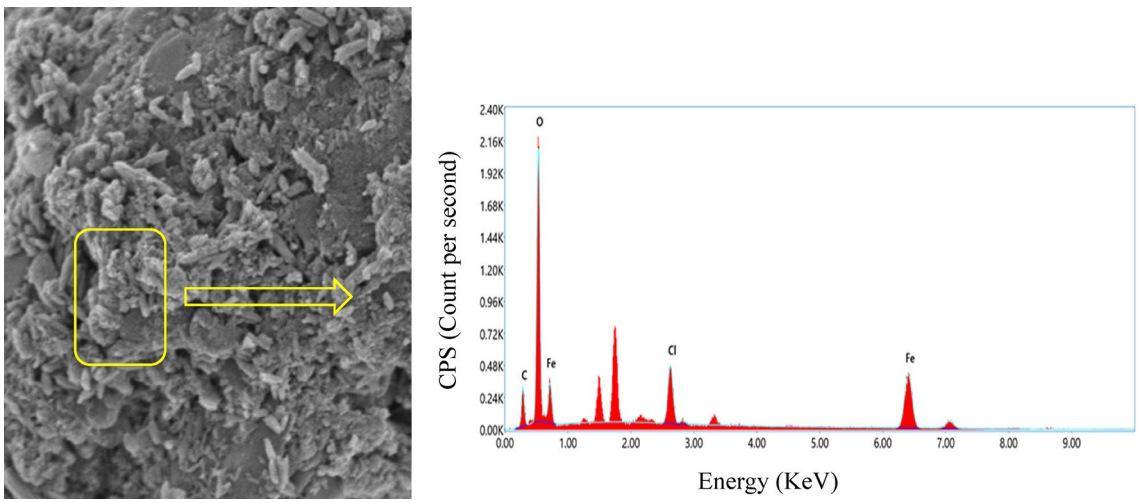

Fig. 8 EDX analysis of *Spirulina* mediated iron oxide nanoparticles

was 59.79% and at pH 12 and 14 it moves to 98.34% and 95.77% respectively. Some of the reasons as stated in the literature for less dye removal efficiency at lower pH are the unfavorable sorption, presence of large no. of H^+ ions and CV dye molecules both of these compete for getting sorbed on the surface of nano-adsorbent. The surface of nano-adsorbent (nanoparticles) is protonated, this also restricts sorption of CV on sorbent (interionic repulsive forces) [31]. Basic pH leads to deprotonation of nano-adsorbent thus as pH increases sorption capacity or dye removal efficiency of nanoadsorbent increases [46]. An experimental study in which cationic and anionic dyes were removed using iron oxide nanoparticles synthesized with the help of *Spirulina platensis* concluded similar results when the impact of pH was studied [31]. Figure 9 demonstrates a change in the efficiency of nano-adsorbent for the removal of CV as pH changes.

3.2.2 Influence of Nano-adsorbent Concentration

The concentration of sorbent greatly influences the sorption of dye on nano-adsorbent. A nano-adsorbent that eliminates a high amount of dye at low doses is said to be an economical sorbent [31]. Six different doses of nano-adsorbent from 10 to 110 mg were used to explore the impact of nano-adsorbent concentration on the removal of crystal violet. As nano-adsorbent concentration increased from 10 to 30 mg removal efficiency increased from 93.69 to 96.12% this is because of the increase in available sorption active site, on which CV can easily sorbed and removed. When nano-adsorbents were used to remove anionic azo acid blue 29 (AB 29) and methylene blue, similar kinds of findings were observed [47]. As nano-adsorbent dose further increased to 50, 70, 90 and 110 mg, removal efficiency decreased to 93.29%, 88.53%, 78.50% and 68.19% respectively. This decrease in removal efficiency is because a high dose of nano-adsorbents leads to clustering thus particle size increases and active surface area is reduced. When iron oxide nanoparticles were synthesized with the help of *Spirulina platensis* and used for the removal of cationic and anionic dyes similar findings were observed [31]. A related kind of finding was reported when CV and tartrazine red dye is removed using iron nano-adsorbent [48, 49]. The influence of nano-adsorbent dose on the removal of CV dye is described in graphical form in Fig. 10.

3.2.3 Sorption Kinetics Analysis

Time reliant variation of pollutant removal is important for practical applications and for calculating sorption rate, contact time, and other rate affecting steps. In the first 10 min, the rate of absorption is high because there is high availability of sorbent and dye molecules [50]. Notably with the passing of time the rate of sorption decrease till the equilibrium condition is attained and this decline is caused by a deficit of inactive binding sites. The final data is subjected to PFORE and PSORE models respectively [51]. PFORE model stated that the rate of change of sorption is parallel to the different equilibrium concentrations [45]. Whereas the PSORE model states that the sorption administering phase is depicted by chemisorption. The linearized model is applied to simulate the kinetics result. The evaluated data is presented in Table 1. The final values of R^2 and K_2 were 0.9966 and 0.010261 respectively. Higher the R^2 value means better the tested fit models.

3.2.4 Sorption Isotherm Analysis

The isothermal analysis is required to offer critical knowledge on sorbent physicochemical characteristics such as

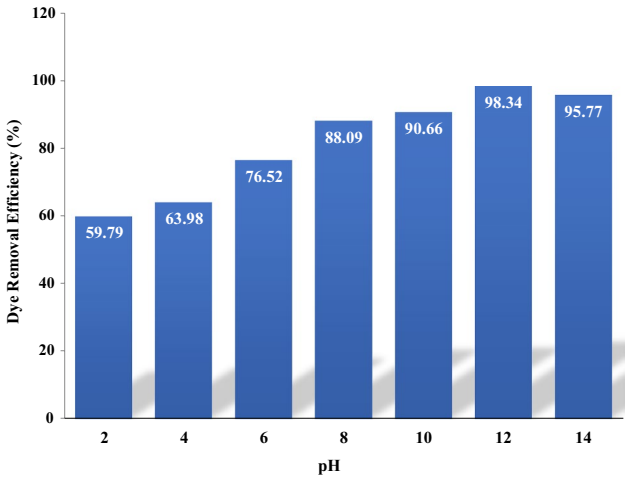

Fig. 9 Percent removal of nano adsorbent for CV dye as a function of pH

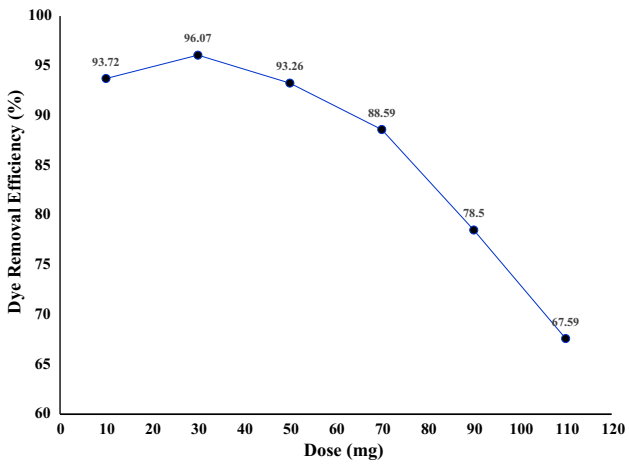

Fig. 10 Influence of nano-adsorbent dose on CV dye removal

Table 1 Uptake kinetics parameters for the sorption of CV dye onto SP- IONPs sorbent

PFORE	
K_1	0.0002
q_e	1
R^2	0.81243
PSORE	
K_2	0.010261
q_e	12.85843
R^2	0.99666

affinity for the pollutant understudy, maximal sorbent capacity, and sorption process. Fundamentally, the LAM, FR, and TK isothermal models were investigated to see which model best explained the mechanism followed by the process of the sorption reaction. Linear graph experimental data and their parameters were tabulated in Table 2. The examined data reported in Table 2 suggested that the LAM isotherm model was better matched to the sorption behaviour of CV onto S-IONPs sorbent rather than others based on the quality of the used models as determined by the obtained R^2 values.

3.2.5 Influence of Temperature

Temperature is one of the important factors that govern the sorption process of crystal violet on nano-adsorbent because temperature influences the diffusion rate of CV molecules [52–55]. To study the influence of temperature on the sorption of CV on nano-adsorbent, 10 different temperature ranges from 35℃ to 80℃ were used. As temperature increases from 35 to 80℃ removal efficiency decreased from 93.13 to 68.6%. Figure 11 demonstrate the impact of temperature on the efficiency of nano-adsorbent for removal of CV dye. A similar kind of finding was reported when algal biomass was grown in distillery industry wastewater. Algal biomass shows the best growth at 35℃ and as temperature increases growth of algal biomass decreases [56].

Table 2 Isothermal parameters for the sorption of CV dye onto SP- IONPs sorbent

Langmuir	
K_L	0.1787
Q_m	55.62
R^2	0.96413
Freundlich	
1/n	0.5383
K_f	9.32
R^2	0.96098

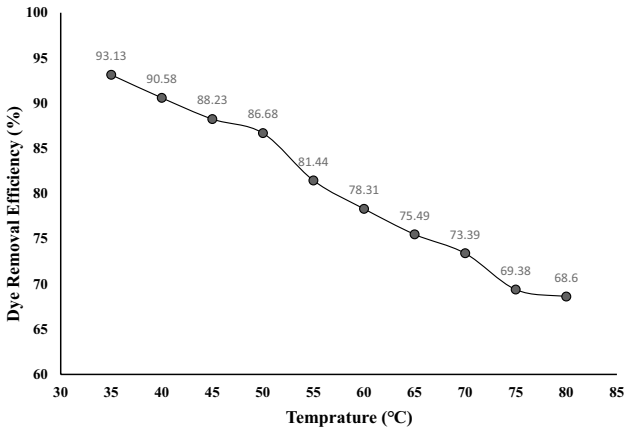

Fig. 11 Impact of temperature on the efficiency of nano-adsorbent for removal of CV dye

4 Conclusion

The current research study describes the *Spirulina's* powder assisted green synthesis, characterisation, and maximum efficiency of nano-adsorbent S-IONPs. The nanoparticles are characterised using FT-IR, XRD, FE-SEM and UV–VIS spectroscopy. The NPs were employed as nano-adsorbents to remove hazardous dye from wastewater. The kinetics and adsorption isotherm were also used to provide important information about the S-IONPs absorption efficiencies towards CV dye. The capacity of S-IONPs to adsorb dye has been tested through various parameters. The dye removal efficiency of nano-adsorbents was found to be highest at pH of 12, the nano-adsorbent dose of 30 mg and temperature of 35 °C. The adsorption isotherm was best fitted in linearized Langmuir theory with r^2 value 0.96413 and q_{max} 55.62 mg/g, whereas the kinetic profile was reported utilizing a pseudo-second order model. The S-IONPs efficiency in sequestering CV dye is found maximum and can effectively remove CV dye from wastewater magnificently.

Acknowledgements We acknowledge the Department of Science & Technology (DST), GoI, New Delhi for providing funding to purchase of Table Top X-ray Diffractometer under the FIST scheme in the Department of Physics, GJUS&T, Hisar and the Central Instrumentation Laboratory, GJUS&T, Hisar.

Declarations

Conflict of interest The authors declare that they have no known competing financial interests or personal relationships that could have appeared to influence the work reported in this paper.

References

1. Mansingh S, Sultana S, Acharya R, Ghosh MK, Parida KM (2020) Efficient photon conversion via double charge dynamics CeO_2–$BiFeO_3$ p–n hetero junction photocatalyst promising toward N2 fixation and phenol–Cr (VI) detoxification. Inorg Chem 59(6):3856–3873
2. Zhang J, Zheng J, Yang W (2020) Co-degradation of ammonia nitrogen and 4-chlorophenol in a photoelectrochemical system by a tandem reaction of chlorine and hydroxyl radicals. Chem Eng Sci 226:115813
3. Liu YC, Li J, Ahn J, Pu J, Rupa EJ, Huo Y, Yang DC (2020) Biosynthesis of zinc oxide nanoparticles by one-pot green synthesis using fruit extract of *Amomum longiligulare* and its activity as a photocatalyst. Optik 218:165245
4. Schweitzer L, Noblet J (2018) Water contamination and pollution. In: Green chemistry. Elsevier, New York, pp 261–290
5. Sellaoui L, Dhaouadi F, Li Z, Cadaval TR Jr, Igansi AV, Pinto LA, Chen Z (2021) Implementation of a multilayer statistical physics model to interpret the adsorption of food dyes on a chitosan film. J Environ Chem Eng 9(4):105516
6. Sekine K, Roskosky M (2018) Emergency response in water, sanitation and hygiene to control cholera in post-earthquake Nepal in 2016. J Water Sanit Hygiene Dev 8(4):799–802
7. Das P, Ghosh S, Ghosh R, Dam S, Baskey M (2018) *Madhuca longifolia* plant mediated green synthesis of cupric oxide nanoparticles: a promising environmentally sustainable material for waste water treatment and efficient antibacterial agent. J Photochem Photobiol B 189:66–73
8. Lü XF, Ma HR, Zhang Q, Du K (2013) Degradation of methyl orange by UV, O 3 and UV/O 3 systems: analysis of the degradation effects and mineralization mechanism. Res Chem Intermed 39(9):4189–4203
9. Katheresan V, Kansedo J, Lau SY (2018) Efficiency of various recent wastewater dye removal methods: a review. J Environ Chem Eng 6(4):4676–4697
10. Islam MA, Ali I, Karim SA, Firoz MSH, Chowdhury AN, Morton DW, Angove MJ (2019) Removal of dye from polluted water using novel nano manganese oxide-based materials. J Water Process Eng 32:100911
11. Abbasi A, Ghanbari D, Salavati-Niasari M, Hamadanian M (2016) Photo-degradation of methylene blue: photocatalyst and magnetic investigation of Fe_2O_3–TiO_2 nanoparticles and nanocomposites. J Mater Sci 27(5):4800–4809
12. Senthilkumaar S, Kalaamani P, Subburaam CV (2006) Liquid phase adsorption of crystal violet onto activated carbons derived from male flowers of coconut tree. J Hazard Mater 136(3):800–808
13. Au W, Pathak S, Collie CJ, Hsu TC (1978) Cytogenetic toxicity of gentian violet and crystal violet on mammalian cells in vitro. Mutat Res 58(2–3):269–276
14. Li Z, Sellaoui L, Gueddida S, Dotto GL, Lamine AB, Bonilla-Petriciolet A, Badawi M (2020) Adsorption of methylene blue on silica nanoparticles: modelling analysis of the adsorption mechanism via a double layer model. J Mol Liq 319:114348
15. Mahmoodi NM, Hayati B, Arami M, Mazaheri F (2010) Single and binary system dye removal from colored textile wastewater by a dendrimer as a polymeric nanoarchitecture: equilibrium and kinetics. J Chem Eng Data 55(11):4660–4668
16. Shaul GM, Holdsworth TJ, Dempsey CR, Dostal KA (1991) Fate of water soluble azo dyes in the activated sludge process. Chemosphere 22(1–2):107–119
17. Aksu Z, Tezer S (2005) Biosorption of reactive dyes on the green alga *Chlorella vulgaris*. Process Biochem 40(3–4):1347–1361
18. Doğar Ç, Gürses A, Açıkyıldız M, Özkan E (2010) Thermodynamics and kinetic studies of biosorption of a basic dye from aqueous solution using green algae Ulothrix sp. Colloids Surf B 76(1):279–285
19. Chowdhury S, Chakraborty S, Saha P (2011) Biosorption of Basic Green 4 from aqueous solution by Ananas comosus (pineapple) leaf powder. Colloids Surf B 84(2):520–527
20. Barka N, Abdennouri M, Makhfouk ME (2011) Removal of Methylene Blue and Eriochrome Black T from aqueous solutions by biosorption on *Scolymus hispanicus* L.: kinetics, equilibrium and thermodynamics. J Taiwan Inst Chem Eng 42(2):320–326
21. Şeker A, Shahwan T, Eroğlu AE, Yılmaz S, Demirel Z, Dalay MC (2008) Equilibrium, thermodynamic and kinetic studies for the biosorption of aqueous lead (II), cadmium (II) and nickel (II) ions on *Spirulina* platensis. J Hazard Mater 154(1–3):973–980
22. Çelekli A, Bozkurt H (2011) Bio-sorption of cadmium and nickel ions using *Spirulina platensis*: kinetic and equilibrium studies. Desalination 275(1–3):141–147
23. Fang L, Zhou C, Cai P, Chen W, Rong X, Dai K, Huang Q (2011) Binding characteristics of copper and cadmium by cyanobacterium *Spirulina platensis*. J Hazard Mater 190(1–3):810–815
24. Rahim A, Çakir C, Ozturk M et al (2021) Chemical characterization and nutritional value of *Spirulina platensis* cultivated in natural conditions of *Chichaoua region* (Morocco). South Afr J Bot.
25. Darezereshki E, Ranjbar M, Bakhtiari F (2010) One-step synthesis of maghemite (γ-Fe2O3) nano-particles by wet chemical method. J Alloys Compd 502(1):257–260
26. Lewis Oscar F, MubarakAli D, Nithya C, Priyanka R, Gopinath V, Alharbi NS, Thajuddin N (2015) One pot synthesis and antibiofilm potential of copper nanoparticles (CuNPs) against clinical strains of *Pseudomonas aeruginosa*. Biofouling 31(4):379–391
27. Chari N, Felix L, Davoodbasha M, Ali AS, Nooruddin T (2017) In vitro and in vivo antibiofilm effect of copper nanoparticles against aquaculture pathogens. Biocatal Agric Biotechnol 10:336–341
28. Shafreen RB, Seema S, Ahamed AP, Thajuddin N, Alharbi SA (2017) Inhibitory effect of biosynthesized silver nanoparticles from extract of Nitzschia palea against curli-mediated biofilm of Escherichia coli. Appl Biochem Biotechnol 183(4):1351–1361
29. Demirezen DA, Yıldız YŞ, Yılmaz Ş, Yılmaz DD (2019) Green synthesis and characterization of iron oxide nanoparticles using Ficus carica (common fig) dried fruit extract. J Biosci Bioeng 127(2):241–245
30. Paiva-Santos AC, Herdade AM, Guerra C, Peixoto D, Pereira-Silva M, Zeinali M, Veiga F (2021) Plant-mediated green synthesis of metal-based nanoparticles for dermopharmaceutical and cosmetic applications. Int J Pharm 597:120311
31. Shalaby SM, Madkour FF, El-Kassas HY, Mohamed AA, Elgarahy AM (2021) Green synthesis of recyclable iron oxide nanoparticles using *Spirulina platensis* microalgae for adsorptive removal of cationic and anionic dyes. Environ Sci Pollut Res 28(46):65549–65572
32. Khan F, Shahid A, Zhu H, Wang N, Javed MR, Ahmad N, et al (2022) Prospects of algae-based green synthesis of nanoparticles for environmental applications. Chemosphere 133571.
33. Ho YS (2004) Selection of optimum sorption isotherm. Carbon 42(10):2115–2116
34. Ho YS, McKay G (1999) Pseudo-second order model for sorption processes. Process Biochem 34(5):451–465
35. Chaudhary S, Kaur Y, Umar A, Chaudhary GR (2016) Ionic liquid and surfactant functionalized ZnO nanoadsorbent for recyclable proficient adsorption of toxic dyes from waste water. J Mol Liq 224:1294–1304
36. Bishnoi S, Kumar A, Selvaraj R (2018) Facile synthesis of magnetic iron oxide nanoparticles using inedible *Cynometra ramiflora*

fruit extract waste and their photocatalytic degradation of methylene blue dye. Mater Res Bull 97:121–127
37. Rahmani R, Gharanfoli M, Gholamin M, Darroudi M, Chamani J, Sadri K, Hashemzadeh A (2020) Plant-mediated synthesis of superparamagnetic iron oxide nanoparticles (SPIONs) using aloe vera and flaxseed extracts and evaluation of their cellular toxicities. Ceram Int 46(3):3051–3058
38. Elgarahy AM, Elwakeel KZ, Elshoubaky GA, Mohammad SH (2019) Microwave-accelerated sorption of cationic dyes onto green marine algal biomass. Environ Sci Pollut Res 26(22):22704–22722
39. Madubuonu N, Aisida SO, Ali A, Ahmad I, Zhao TK, Botha S, Ezema FI (2019) Biosynthesis of iron oxide nanoparticles via a composite of Psidium guavaja-Moringa oleifera and their antibacterial and photocatalytic study. J Photochem Photobiol B 199:111601
40. Kouhbanani M, Beheshtkhoo N, Taghizadeh S, Amani A, Alimardani V (2019) One-step green synthesis and characterization of iron oxide nanoparticles using aqueous leaf extract of *Teucrium polium* and their catalytic application in dye degradation. Adv Nat Sci 10:015007. https://doi.org/10.1088/2043-6254/aafe74
41. Lakshmnarayanan S, Shereen MF, Niraimathi KL, Brindha P, Arumugam A (2021) One-pot green synthesis of iron oxide nanoparticles from Bauhinia tomentosa: characterization and application towards synthesis of 1, 3 diolein. Sci Rep 11(1):1–13
42. Jagathesan G, Rajiv P (2018) Biosynthesis and characterization of iron oxide nanoparticles using *Eichhornia crassipes* leaf extract and assessing their antibacterial activity. Biocatal Agric Biotechnol 13:90–94
43. Pai S, Kini SM, Narasimhan MK, Pugazhendhi A, Selvaraj R (2021) Structural characterization and adsorptive ability of green synthesized Fe3O4 nanoparticles to remove Acid blue 113 dye. Surf Interfaces 23:100947
44. Demirezen DA, Yıldız YŞ, Yılmaz DD (2019) Amoxicillin degradation using green synthesized iron oxide nanoparticles: kinetics and mechanism analysis. Environ Nanotechnol Monit Manag 11:100219
45. Rigueto CVT, Piccin JS, Dettmer A et al (2020) Water hyacinth (*Eichhornia crassipes*) roots, an amazon natural waste, as an alternative biosorbent to uptake a reactive textile dye from aqueous solutions. Ecol Eng 150:105817
46. Mittal H, Al Alili A, Morajkar PP, Alhassan SM (2021) Graphene oxide crosslinked hydrogel nanocomposites of xanthan gum for the adsorption of crystal violet dye. J Mol Liq 323:115034
47. Marrakchi F, Hameed BH, Hummadi EH (2020) Mesoporous biohybrid epichlorohydrin crosslinked chitosan/carbon–clay adsorbent for effective cationic and anionic dyes adsorption. Int J Biol Macromol 163:1079–1086
48. Barizão A, Silva M, Andrade M, Brito F, Gomes R, Bergamasco R (2019) Green synthesis of iron oxide nanoparticles for tartrazine and bordeaux red dye removal. J Environ Chem Eng 8:103618. https://doi.org/10.1016/j.jece.2019.103618
49. Rawat S, Samreen K, Nayak AK, Singh J, Koduru JR (2021) Fabrication of iron nanoparticles using Parthenium: a combinatorial eco-innovative approach to eradicate crystal violet dye and phosphate from the aqueous environment. Environ Nanotechnol Monit Manag 15:100426
50. Prajapati AK, Mondal MK (2021) Novel green strategy for CuO–ZnO–C nanocomposites fabrication using marigold (Tagetes spp.) flower petals extract with and without CTAB treatment for adsorption of Cr(VI) and Congo red dye. J Environ Manag 290:112615
51. Jabli M, Almalki SG, Agougui H (2020) An insight into methylene blue adsorption characteristics onto functionalized alginate bio-polymer gel beads with λ-carrageenan-calcium phosphate, carboxymethyl cellulose, and celite 545. Int J Biol Macromol 156:1091–1103
52. Pugazhendhi A, Boovaragamoorthy GM, Ranganathan K, Naushad M, Kaliannan T (2018) New insight into effective biosorption of lead from aqueous solution using *Ralstonia solanacearum*: characterization and mechanism studies. J Clean Prod 174:1234–1239
53. Rajumon R, Anand JC, Ealias AM, Desai DS, George G, Saravanakumar MP (2019) Adsorption of textile dyes with ultrasonic assistance using green reduced graphene oxide: an in-depth investigation on sonochemical factors. J Environ Chem Eng 7(6):103479
54. Mona S, Kaushik A, Kaushik CP (2011) Biosorption of reactive dye by waste biomass of *Nostoc linckia*. Ecol Eng 37:1589–1594
55. Mona S, Kaushik A, Kaushik CP (2011) Waste biomass of *Nostoc linckia* as adsorbent of crystal violet dye: optimization based on statistical model. Int Biodeterior Biodegrad 65(3):513–521
56. Ahmad S, Kothari R, Shankarayan R, Tyagi VV (2020) Temperature dependent morphological changes on algal growth and cell surface with dairy industry wastewater: an experimental investigation. Biotech 10(1):1–12

Authors and Affiliations

Santosh Bhukal[1] · Anuj Sharma[1] · Rishi[1] · Divya[1] · Sumit Kumar[1] · Bansal Deepak[1,2] · Kaushik Pal[3] · Sharma Mona[1,4]

✉ Sharma Mona
monasharma.gjust@gmail.com

[1] Department of Environmental Science & Engineering, Guru Jambheshwar University of Science & Technology, Hisar, Haryana 125001, India

[2] JBM Group, Gurugram, Haryana 122001, India

[3] University Centre for Research and Development (UCRD), Department of Physics, Chandigarh University, Mohali, Gharuan, Punjab 140413, India

[4] Department of Environmental Studies, School of Interdisciplinary and Applied Sciences, Central University of Haryana, Mahendergarh, Haryana 123031, India